

Deflection of an Elliptically-Loaded Vortex Sheet by a Flat Plate

by Jason O. Archer
University of New Mexico
Department of Mathematics and Statistics
advised by Dr. Monika Nitsche

Abstract

We investigate the behavior of fluid flows using computer simulations. Specifically, we simulate the flow of fluid induced by an elliptically loaded vortex sheet and a stationary flat plate, using a point-vortex approximation. In our simulations, we modify the distance from the vortex sheet to the plate, the angle of the plate relative to the sheet, and a smoothing parameter. We study the effects these parameters have on the evolution of the vortex sheet, the trajectories of the endpoints of the sheet, the trajectories of the leftmost and rightmost inflection points of the sheet, the trajectory of the midpoint of the sheet, and the trajectories of two point vortices placed so as to approximate the total sheet, as these are all deflected by the plate. We accomplish this simulation by evolving the locations of point vortices forward in time using a set of ODE's under 4th-order Runge-Kutta approximation.

I. Introduction




 Wake Vortex Study at Wallops Island
NASA Langley Research Center 5/4/1990 Image # EL-1996-00130

Fig. 1: The airplane's trailing wingtip vortices are illustrated here with colored smoke.
Source: NASA

Download source: http://commons.wikimedia.org/wiki/File:Airplane_vortex.jpg

When airplanes fly through the air, they leave downward-moving vortex flows trailing their path, as shown in Figure 1. These vortex flows behind a large airplane can cause turbulence for other smaller airplanes. Preventing such flows from affecting following airplanes is the primary reason airports limit times between takeoffs and landings. However, crashes still sometimes occur when an aircraft flies into another aircraft's path too soon; one example is American Airlines Flight 587 in November 12, 2001.

We now provide a short description of how trailing vortices are created. When air (or another fluid) flows past an airplane wing (or another similar interruption), two boundary layers of vorticity form on either side of this wing due to the friction of this wing moving relative to the fluid. The friction drags particles of air along with the wing as it moves through the air. As a result, the fluid velocity at the surface of the wing equals the very large wing velocity, but the fluid velocity is very small a little further away from the wing. This means there are large gradients of velocity in the fluid; see Figure 2b.

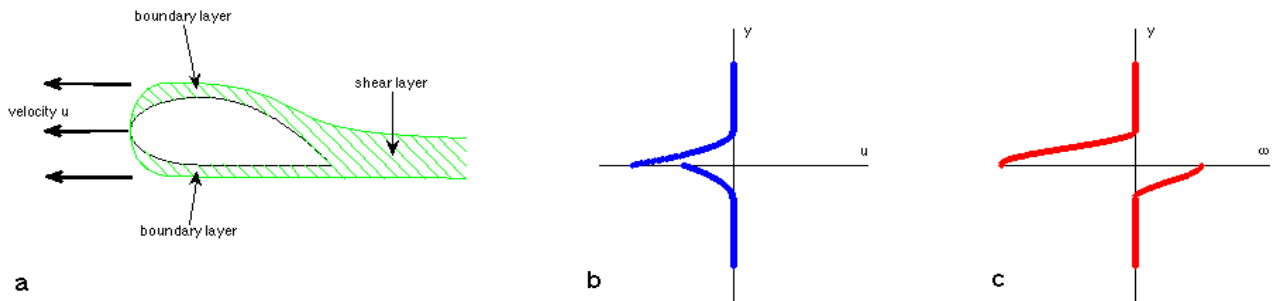


Fig. 2: a: Sketch of boundary and shear layers trailing a wing (the wing is traveling left in the diagram, as is the air it drags); b: Sketch of tangential velocity vertical profile of fluid trailing same wing; c: Sketch of vorticity vertical profile of fluid trailing same wing.

When these boundary layers finally meet at the trailing edge of the wing, they form a shear layer, which is a thin layer of vorticity in the fluid; see Figure 2a. Vorticity ω is defined to be the curl of the velocity vector field \vec{u} , and measures the amount of rotation of the fluid. This can be seen from the following application of Stokes's theorem (or Green's theorem, when applied in two dimensions). Assuming \vec{u} to be 2-dimensional,

$$\vec{u} = (u(x, y), v(x, y), 0) \rightarrow \vec{\omega} = \vec{\nabla} \times \vec{u} = (0, 0, v_x - u_y) \rightarrow \omega = v_x - u_y;$$

$$\rightarrow \int_{\partial D} \vec{u} \cdot \hat{T} ds = \int_{\partial D} u dy - v dx = \iint_D (v_x - u_y) dx \cdot dy = \iint_D (v_x - u_y) dA = \iint_D \vec{\omega} \cdot \hat{n} dA = \iint_D \omega dA;$$

The integral on the left-hand side is a circulation integral which measures the total tangential velocity around a closed counterclockwise curve; if this integral $\int_{\partial D} \vec{u} \cdot \hat{T} ds$ is nonzero, then there is rotation in the fluid. What Green's theorem tells us is that if the vorticity ω is nonzero, then the right-hand side integral $\iint_D \omega dA$ is nonzero, which means that the left-hand side integral is nonzero, which means there is rotation in the fluid. In short, if $\omega \neq 0$, then there is rotation.

For the fluid flow past the wing in Figure 2, we explained why the velocity gradients are quite large close to the wing; therefore, the vorticity is large in that region. In particular, if the flow is practically parallel to the wing, we can say

$$v \approx 0 \rightarrow v_x \approx 0 \rightarrow \omega \approx -u_y$$

as illustrated in Figure 2c.

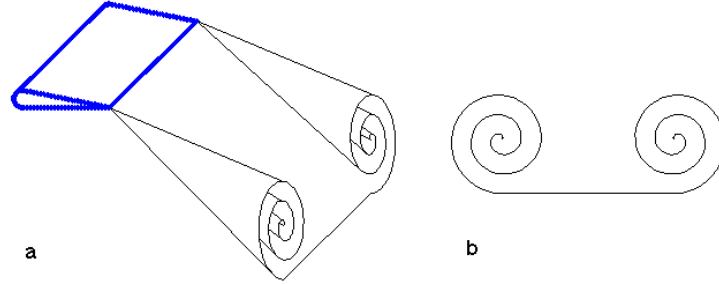


Fig. 3: a: Sketch of three-dimensional view of shear layer (thin outline) shed from the trailing edge of a moving wing (thick outline). b: Sketch of parallel cross-section of shear layer.

Changing our perspective, we note that the actual shear layer is 3-dimensional, as shown in Figure 3a. If we look at a cross-section of the shear layer parallel to the wing, we can more clearly see the vortex sheet in space; see Figure 3b. We compute the motion of the sheet from the perspective shown in Figure 3b by assuming planar symmetry in this plane.

A common method (used by Krasny^{2,3,4}) of modeling a shear layer is with a thin sheet of vorticity, or “vortex sheet,” which approximates this shear layer with a layer of zero thickness and infinite vorticity, such that the product of thickness and vorticity remains constant. In our simulation, we use this vortex sheet model to approximate the trailing flow past an aircraft wing, in three dimensions. The strength of the sheet is the discontinuity in the tangential velocities from the top to the bottom of the sheet; see Figure 2b.

We compute the evolution of this sheet of vorticity using a set of two-dimensional point vortex approximations in the plane, a model of three-dimensional space which uses two spatial dimensions perpendicular to the direction of movement of the wing and a time dimension parallel to that direction. In keeping with the work of Krasny^{2,3,4}, we use 64-bit double-precision numbers for these calculations; numbers with lower precision have been shown to yield less accurate computations.

Just as Krasny³ did, we use an elliptically-loaded vortex sheet to simulate our fluid flows. This means that we set the strength of the individual point vortices comprising the vortex sheet to be a sinusoidal function of position. This strength w is derived from the jump discontinuity in velocity from the bottom to the top edges of the vortex sheet, which gives us the following elliptical formula;

$$\frac{d\Gamma}{d\alpha} = w; x^2 + w^2 = 1 \rightarrow w = \sqrt{1 - x^2}$$

Since the initial number of point vortices is not enough to accurately represent the vortex sheet as time progresses, we place more as needed via Lagrange polynomial interpolation.

We insert a flat, rigid, solid plate into the simulation, below the initial vortex sheet location, past which the vortex sheet flows. We define as a spatial boundary condition that the vortex sheet may not flow through it, only past it. We simulate this plate as a set of point vortices with a total combined circulation of zero, but individual regions must have nonzero differential circulations which are computed using linear algebra. The total circulation around the vortex sheet is also zero, but individual segments must also have nonzero differential circulations, which are more simply calculated as a sinusoidal function, which we describe below. We step the simulation forward in time using 4th-order Runge-Kutta approximation.

In addition to a basic simulation with predefined parameters, we vary the relative vertical distance d between the plate and the sheet, the approximation parameter δ , and the angle of plate incline ϕ ; see Figure 4. The approximation parameter δ is commonly used in fluid mechanics problems (e.g. Krasny^{1, 3, 4} and Nitsche^{1, 6, 7}) in order to provide close approximations to actual solutions, when actual solutions cannot be found by numerical computation.

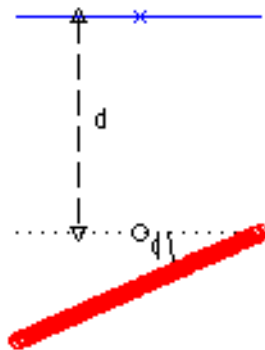


Fig. 4: Diagram of Parameters: vertical distance d , and plate angle ϕ . Origin at O , vortex sheet center at x .

In the future, we would like to examine what happens to the flow when the plate is

- 1) offset with some horizontal displacement,
- 2) no longer stationary, but oscillating with certain amplitudes and frequencies, and
- 3) no longer flat, but curved or angled.

We would also like to test other interpolation schemes (e.g. using Chebyshev polynomials) to determine their impact on the simulation. Additionally, we would like to examine the exact relationship of the plate angle to the vortex deflection angle.

We perform calculations on an Apple 2 GHz Intel Core Duo iMac with 512 MB of 667 MHz RAM, using Mac OS X Tiger 10.4.11. We utilize the g95 Fortran 95 compiler with routines from LAPACK 3.2.1 with BLAS, using X11 1.1.3 - XFree86 4.4.0, writing code in Xcode 2.4, displaying graphs with the aid of MATLAB 7.4.0.287 (R2007a) Student Version.

We begin in §II by reviewing some literature relevant to fluid mechanics. Then, in §III, we will discuss the governing equations of our simulation, both in a continuous and discrete sense. Afterward, in §IV, we will examine the results of our simulations, both under basic and varied conditions.

II. Literature Review

A. *A numerical study of vortex ring formation at the edge of a circular tube*¹

In this paper, Nitsche and Krasny simulate the evolution of the vorticity shed from a moving piston out of a circular tube opening, investigating the vortex sheet behavior for varying values of a smoothing parameter. They compare this behavior with real-world experimental data, and contrast it against established two-dimensional theories.

B. *A study of singularity formation in a vortex sheet by the point vortex approximation*²

In this paper, Krasny simulates the time progression of vortex sheet equations to study singularities in a periodically bound vortex sheet; these singularities are real, but their presence ruins computational accuracy. He discusses the usage of spectral filtering and straight-line interpolation in order to approximate the effects of this singularity, while preserving computational accuracy as much as possible.

C. *Computation of vortex sheet roll-up in the Trefftz plane*³

In this paper, Krasny simulates the evolution of vortex sheets on the Trefftz plane, using a smoothing parameter. He examines the tip region of the vortex sheet as it deforms for large time. He examines variations in the vortex sheet as he alters the number of point vortices used to approximate the sheet, the size of the time step, the smoothing parameter, and machine precision. He compares observed behavior with established theories.

D. *Desingularization of Periodic Vortex Sheet Roll-up*⁴

In this paper, Krasny simulates the modification of vortex sheet equations to remove singularities in a periodically bound vortex sheet; these singularities are real, but we cannot compute the exact solution to the movement of the vortex sheet past the time of the singularities' formation. In order to compute past this time, he discusses the usage of a smoothing parameter to regularize the equations, as well as the usage of higher machine precision and spectral filtering in order to reduce this smoothing parameter as close to zero as possible. It is not yet clear what the exact relation is between the solutions of the exact equations and that of their regularized forms, past the time of singularity formation.

E. *Minicourse 4: An Introduction to Fluid Dynamics*⁵

In this instructional paper, Nitsche introduces basic fluid mechanics concepts, such as velocity fields, particle trajectories, vorticity, circulation, point vortex motion, viscosity, compressibility, Euler's equations, Bernoulli's Theorem, potential flows, and the Navier-Stokes equations, as well as other concepts.

F. *Scaling properties of vortex ring formation at a circular tube opening*⁶

In this paper, Nitsche simulates the vorticity shed from a moving piston out of a circular tube opening, investigating the vortex sheet behavior for varying values of piston velocity and of a smoothing

parameter, and comparing this behavior with established theories.

G. *Vortex Dynamics*⁷

In this instructional paper, Nitsche discusses vortex motion; the relevant mathematical theory, various applications and examples, and numerical methods for computation.

H. *private communication*⁸

In this private communication, Pullin makes a conjecture about the nature of vortex sheet behavior past a critical time, when singularities of infinite curvature develop in the sheet. He states that beyond this time, the vortex sheet is a double branched spiral with an infinite number of turns.

III. Governing Equations

The fluid flows are governed by the differential equations of inviscid incompressible 2-dimensional fluid flows. The initial condition for the location of the free vortex sheet (i.e. vortex sheet that moves with some induced fluid velocity) is a straight line, the initial condition for the vortex sheet strength is elliptical loading, the initial condition for the location of the interfering plate is another straight line below the vortex sheet, and the boundary conditions at the interfering plate prevent fluid permeability. We use the initial and boundary conditions of the plate to determine the strength of the plate.

A. *Background*

We begin by introducing Euler's equations of inviscid incompressible flow;

$$\begin{cases} \frac{D\rho}{Dt} = 0 \\ \rho \frac{D\vec{u}}{Dt} = -\vec{\nabla} p \\ \vec{\nabla} \cdot \vec{u} = 0 \\ \vec{u} \cdot \hat{n} = \vec{U}_{wall} \cdot \hat{n} \text{ on } \partial D \end{cases}$$

where ρ is the fluid density, \vec{u} is the fluid velocity, \vec{U}_{wall} is the wall/boundary velocity (which is equal to 0 if the wall is stationary), and p is the fluid pressure. The D/Dt operator is the material derivative, defined as follows;

$$\frac{D}{Dt} = \frac{\partial}{\partial t} + \vec{u} \cdot \vec{\nabla}$$

We know from vector calculus that for incompressible 2-dimensional flows there exists a streamfunction $\psi(x, y, t)$ whose level curves are streamlines of the flow. The following formulas apply to the streamfunction;

$$\begin{aligned}\frac{\partial \psi}{\partial x} &= -v, \quad \frac{\partial \psi}{\partial y} = u; \\ \nabla^2 \psi &= -v_x + u_y = -\omega\end{aligned}$$

Therefore, if we know the vorticity, its negative is the Laplacian of the streamfunction, and it solves a Poisson equation under Dirichlet boundary conditions, when $\psi=0$ on the boundary of the domain. According to Green's functions of the Poisson equation, on the R^2 domain (for which the boundary is at infinity),

$$\psi = \frac{-1}{2\pi} \int \omega(\vec{x}') \ln |\vec{x} - \vec{x}'| d\vec{x}' \approx \frac{-1}{2\pi} \int \ln |\vec{x} - \vec{x}'| d\Gamma$$

Taking the above derivatives of this equation, we yield the 2-dimensional version of the Biot-Savart law;

$$u = \psi_y = \frac{-1}{2\pi} \int \frac{x-x'}{(x-x')^2 + (y-y')^2} d\Gamma; \quad v = -\psi_x = \frac{1}{2\pi} \int \frac{y-y'}{(x-x')^2 + (y-y')^2} d\Gamma$$

B. Nondimensionalization

To permit computation, we nondimensionalize our parameters according to standard units of length and circulation. We use the half-length of the plate and the circulation of half of the vortex sheet as standard units of measurement to develop common space, time, and velocity scales as follows;

$$\begin{aligned}[L_{1/2}] &= \text{length}; \quad [\Gamma_{1/2}] = \frac{\text{length}^2}{\text{time}}; \\ \text{Length Scale} &= L_{1/2}; \quad \text{Time Scale} = \frac{L_{1/2}^2}{\Gamma_{1/2}}; \quad \text{Velocity Scale} = \frac{\Gamma_{1/2}}{L_{1/2}}\end{aligned}$$

We then apply these scales as follows;

$$\tilde{x} = \frac{x}{L_{1/2}}; \quad \tilde{y} = \frac{y}{L_{1/2}}; \quad \tilde{t} = \frac{t}{\left(\frac{L_{1/2}^2}{\Gamma_{1/2}}\right)}; \quad \tilde{u} = \frac{u}{\left(\frac{\Gamma_{1/2}}{L_{1/2}}\right)}; \quad \tilde{v} = \frac{v}{\left(\frac{\Gamma_{1/2}}{L_{1/2}}\right)}$$

C. Continuous Vortex Sheet

The velocity at every point in the field can be written as an ODE using the Biot-Savart law as

$$\tilde{u}_k(\tilde{t}, \tilde{x}) = \frac{1}{2\pi} \int \frac{(-(\tilde{y} - \tilde{y}_k), \tilde{x} - \tilde{x}_k)}{(\tilde{x} - \tilde{x}_k)^2 + (\tilde{y} - \tilde{y}_k)^2} d\tilde{\Gamma} + \overline{\nabla} \tilde{\Phi} = \frac{1}{2\pi} \int \frac{(-(\tilde{y} - \tilde{y}_k), \tilde{x} - \tilde{x}_k)}{(\tilde{x} - \tilde{x}_k)^2 + (\tilde{y} - \tilde{y}_k)^2} d\tilde{\Gamma} + \overline{\nabla} \tilde{\Phi}$$

where $\overline{\nabla} \tilde{\Phi}$ is a potential flow added such that no fluid passes through the interfering plate i.e. the normal component of the fluid velocity on the plate is exactly zero. We represent this boundary

condition as follows;

$$\left(\sum_k \vec{u}_k \right) \cdot \hat{n} = 0, \hat{n} = (-\sin \varphi, \cos \varphi)$$

where \hat{n} is the unit vector normal to the plate. (This condition is of similar form to the 4th Euler equation of incompressible flow.) At any given point \vec{x} on the sheet, the circulation at that point is

$$\tilde{\Gamma}(\alpha) = \sin \alpha$$

where α is the “angle” parameter of the vortex sheet, on a domain $\alpha = [0, \pi]$, defined by the relation

$$\vec{x}(\alpha, 0) = (-\cos \alpha, 0)$$

We take the y-component of the vortex sheet locations to be 0 because we can set the angle of the interfering plate (described later in further detail) to be at any location oriented at any angle we desire, relative to the vortex sheet; this allows us to create any practical orientation we require.

D. Discrete Vortex Sheet

We discretize the vortex sheet using a finite number of point vortices with corresponding values of the parameter α . We used an elliptically-loaded vortex sheet, placing these vortices according to the placement formula

$$\vec{x}_k(\alpha_k, 0) = (-\cos \alpha_k, 0)$$

1. Point Vortex Approximation

Since we cannot calculate continuous quantities on a computer, we approximate the vortex sheet as a set of point vortices; according to Nitsche,⁵ the k'th individual point vortex of the vortex sheet induces a velocity of

$$\vec{u}_k(\tilde{t}, \vec{x}) = \left(\frac{\Delta \tilde{\Gamma}_k}{2\pi} \frac{-(\tilde{y} - \tilde{y}_k(\alpha_k, \tilde{t}))}{(\tilde{x} - \tilde{x}_k(\alpha_k, \tilde{t}))^2 + (\tilde{y} - \tilde{y}_k(\alpha_k, \tilde{t}))^2}, \frac{\Delta \tilde{\Gamma}_k}{2\pi} \frac{\tilde{x} - \tilde{x}_k(\alpha_k, \tilde{t})}{(\tilde{x} - \tilde{x}_k(\alpha_k, \tilde{t}))^2 + (\tilde{y} - \tilde{y}_k(\alpha_k, \tilde{t}))^2} \right);$$

where k is a number between 0 and the total number of point vortices, $\tilde{x}_k(\alpha_k, \tilde{t})$ is the x-location of the k'th vortex at time \tilde{t} , $\tilde{y}_k(\alpha_k, \tilde{t})$ is the y-location of the k'th vortex at time \tilde{t} , and $\Delta \tilde{\Gamma}_k$ is the circulation/strength of the k'th vortex, calculated as follows;

$$\Delta \tilde{\Gamma}_k = w_k \cdot \Delta \alpha_k = \frac{d \tilde{\Gamma}}{d \alpha} \Big|_k \cdot \Delta \alpha_k = \cos(\alpha_k) \cdot \Delta \alpha_k;$$

$$\tilde{x}_k = -\cos(\alpha_k) \rightarrow \tilde{\Gamma}_k = \sqrt{1 - \tilde{x}_k^2} = \sin(\alpha_k) \rightarrow \Delta \tilde{\Gamma}_k = \frac{\tilde{\Gamma}_{k+1} - \tilde{\Gamma}_{k-1}}{2} = \frac{\sin \alpha_{k+1} - \sin \alpha_{k-1}}{2}$$

$$= \frac{\sin \alpha_{k+1} - \sin \alpha_{k-1}}{2 \Delta \alpha_k} \cdot \Delta \alpha_k \approx \cos(\alpha_k) \cdot \Delta \alpha_k$$

The final approximate equality holds true, since the left-hand side is the right-hand side rendered as a first-order finite-difference derivative approximation formula.

The formula for $\tilde{u}_k(\tilde{t}, \tilde{x})$ causes a problem when we attempt to calculate the velocity induced on any given point vortex by itself, since this would involve dividing by zero.

We start with $K+1=1000$ vortices (numbered 0 through 999) on our vortex sheet; using fewer vortices seems to provide very little computational advantage, and using more vortices takes up too much computing time.

The initial vortex sheet has singularities at the tips at time $\tilde{t}=0$. This is because

$$\tilde{\Gamma}_k \sim \sqrt{1 - \tilde{x}_k^2} \rightarrow \frac{d \tilde{\Gamma}}{d \tilde{x}} \Big|_k \sim \frac{\tilde{x}_k}{\sqrt{1 - \tilde{x}_k^2}}$$

thus singularities occur when \tilde{x}_k approaches ± 1 . Therefore, we must regularize the equations to compute past this time without singularities. We use an approximation parameter δ , which we try to make very small. We regularize the velocity ODE with this small parameter δ as follows;

$$\tilde{u}_k(\tilde{t}, \tilde{x}) = \left(\frac{\Delta \tilde{\Gamma}_k}{2 \pi} \frac{-(\tilde{y} - \tilde{y}_k(\alpha_k, \tilde{t}))}{(\tilde{x} - \tilde{x}_k(\alpha_k, \tilde{t}))^2 + (\tilde{y} - \tilde{y}_k(\alpha_k, \tilde{t}))^2 + \delta^2}, \frac{\Delta \tilde{\Gamma}_k}{2 \pi} \frac{\tilde{x} - \tilde{x}_k(\alpha_k, \tilde{t})}{(\tilde{x} - \tilde{x}_k(\alpha_k, \tilde{t}))^2 + (\tilde{y} - \tilde{y}_k(\alpha_k, \tilde{t}))^2 + \delta^2} \right)$$

in keeping with the work of Krasny^{1,3,4} and Nitsche^{1,6,7}. This enables us to set the velocity induced on any given point vortex by itself to be zero in our calculations. We assume that the exact solution to our equations of fluid motion can be found in the limit as this small parameter δ approaches zero.

According to the conjectures of Pullin⁸, the vortex sheet is a double-branched spiral with infinitely many turns past the critical time, and that these spirals vanish in size as the critical time is approached from above.

2. Plate Insertion

We insert a flat plate into the simulation, such that the point on the plate closest to the vortex sheet is a horizontal distance d away from the sheet; this alters the velocity calculations. We also approximate the plate as a set of $I+1=600$ point vortices (numbered 0 through 599), all of which remain stationary throughout the whole simulation (unlike the vortices on the fluid vortex sheet).

Each of these point vortices corresponds to a value of the parameter β as follows;

$$\vec{\tilde{x}}_p(\beta) = (\cos \beta \cos \varphi, \cos \beta \sin \varphi - |\sin \varphi|) \nabla \beta = [0, \pi]$$

or, discretely,

$$\vec{\tilde{x}}_p(\beta_i) = (\cos \beta_i \cos \varphi, \cos \beta_i \sin \varphi - |\sin \varphi|) \nabla i = [0, I]$$

where $\vec{\tilde{x}}_p(\beta_i)$ is the position vector of the i'th vortex on the plate, and φ is the angle made by the plate relative to the horizontal. To calculate the strength of these point vortices, we must consider that no fluid may flow through the plate. We render this mathematically with the following equation;

$$\vec{\tilde{u}}_{total} \cdot \hat{n} = 0$$

or

$$\left(\sum_k \vec{\tilde{u}}_k + \sum_i \vec{\tilde{u}}_i \right) \cdot \hat{n} = 0$$

Since the velocity contributions of each point vortex of the plate on the sheet and of each point vortex of the sheet on every other point vortex on the sheet must be added to obtain the total velocity, we get the following ODE, which is just a discretized and regularized version of the Biot-Savart law;

$$\vec{\tilde{u}}_{total}(\tilde{t}, \tilde{x}) = \frac{1}{2\pi} \left[\sum_k \frac{(-(\tilde{y} - \tilde{y}_k), \tilde{x} - \tilde{x}_k)}{(\tilde{x} - \tilde{x}_k)^2 + (\tilde{y} - \tilde{y}_k)^2 + \delta^2} \Delta \tilde{\Gamma}_k + \sum_i \frac{(-(\tilde{y} - \tilde{y}_i), \tilde{x} - \tilde{x}_i)}{(\tilde{x} - \tilde{x}_i)^2 + (\tilde{y} - \tilde{y}_i)^2} \Delta \tilde{\Gamma}_i \right]$$

By evaluating the above two equations at each midpoint between two adjacent point vortices, we derive an incomplete system of equations as follows;

$$\begin{aligned} & - \left(\sin \varphi \sum_{k=0}^K \frac{m\tilde{y}_j - \tilde{y}_k}{(m\tilde{x}_j - \tilde{x}_k)^2 + (m\tilde{y}_j - \tilde{y}_k)^2 + \delta^2} \Delta \tilde{\Gamma}_k + \cos \varphi \sum_{k=0}^K \frac{m\tilde{x}_j - \tilde{x}_k}{(m\tilde{x}_j - \tilde{x}_k)^2 + (m\tilde{y}_j - \tilde{y}_k)^2 + \delta^2} \Delta \tilde{\Gamma}_k \right) \\ & = \sum_{i=0}^I \frac{\sin \varphi (m\tilde{y}_j - \tilde{y}_i) + \cos \varphi (m\tilde{x}_j - \tilde{x}_i)}{(m\tilde{x}_j - \tilde{x}_i)^2 + (m\tilde{y}_j - \tilde{y}_i)^2} \Delta \tilde{\Gamma}_i \quad \forall j = [0, I-1] \end{aligned}$$

where $(m\tilde{x}_j, m\tilde{y}_j)$ is the location of the j'th midpoint of the plate, which is halfway between the i'th and (i+1)'th points of the plate. To make this system complete, we must recall our condition that the total circulation of the plate is 0; this yields the equation

$$\sum_i \Delta \tilde{\Gamma}_i = 0$$

The previous two equations, taken together, form a complete linear system, with which we can compute all vortex strengths $\Delta \tilde{\Gamma}_i$ as follows;

$$\begin{pmatrix} \frac{\sin \varphi(\tilde{y}_0 - \tilde{y}_0) + \cos \varphi(\tilde{x}_0 - \tilde{x}_0)}{(\tilde{x}_0 - \tilde{x}_0)^2 + (\tilde{y}_0 - \tilde{y}_0)^2} & \dots & \frac{\sin \varphi(\tilde{y}_0 - \tilde{y}_l) + \cos \varphi(\tilde{x}_0 - \tilde{x}_l)}{(\tilde{x}_0 - \tilde{x}_l)^2 + (\tilde{y}_0 - \tilde{y}_l)^2} \\ \vdots & \ddots & \vdots \\ \frac{\sin \varphi(\tilde{y}_{l-1} - \tilde{y}_0) + \cos \varphi(\tilde{x}_{l-1} - \tilde{x}_0)}{(\tilde{x}_{l-1} - \tilde{x}_0)^2 + (\tilde{y}_{l-1} - \tilde{y}_0)^2} & \dots & \frac{\sin \varphi(\tilde{y}_{l-1} - \tilde{y}_l) + \cos \varphi(\tilde{x}_{l-1} - \tilde{x}_l)}{(\tilde{x}_{l-1} - \tilde{x}_l)^2 + (\tilde{y}_{l-1} - \tilde{y}_l)^2} \\ 1 & \dots & 1 \end{pmatrix} \begin{pmatrix} \Delta \tilde{T}_0 \\ \vdots \\ \vdots \\ \Delta \tilde{T}_l \end{pmatrix} = - \begin{pmatrix} \sum_{k=0}^K \frac{\sin \varphi(\tilde{y}_0 - \tilde{y}_k) + \cos \varphi(\tilde{x}_0 - \tilde{x}_k)}{(\tilde{x}_0 - \tilde{x}_k)^2 + (\tilde{y}_0 - \tilde{y}_k)^2 + \delta^2} \Delta \tilde{T}_k \\ \vdots \\ \sum_{k=0}^K \frac{\sin \varphi(\tilde{y}_{l-1} - \tilde{y}_k) + \cos \varphi(\tilde{x}_{l-1} - \tilde{x}_k)}{(\tilde{x}_{l-1} - \tilde{x}_k)^2 + (\tilde{y}_{l-1} - \tilde{y}_k)^2 + \delta^2} \Delta \tilde{T}_k \\ 0 \end{pmatrix}$$

3. Time Steps

We then use 4th-order Runge-Kutta approximation to step forward in time according to this calculated velocity, in order to examine the behavior of the vortex sheet over a period of time.

$$\begin{cases} \vec{k}_1 = \vec{u}(\tilde{t}, \tilde{x}); \\ \vec{k}_2 = \vec{u}\left(\tilde{t} + \frac{\Delta \tilde{t}}{2}, \tilde{x} + \frac{\Delta \tilde{t}}{2} \vec{k}_1\right); \\ \vec{k}_3 = \vec{u}\left(\tilde{t} + \frac{\Delta \tilde{t}}{2}, \tilde{x} + \frac{\Delta \tilde{t}}{2} \vec{k}_2\right); \\ \vec{k}_4 = \vec{u}(\tilde{t} + \Delta \tilde{t}, \tilde{x} + (\Delta \tilde{t}) \vec{k}_3); \\ \tilde{x}(\tilde{t} + \Delta \tilde{t}) = \tilde{x}(\tilde{t}) + \frac{\Delta \tilde{t}}{6} (\vec{k}_1 + 2\vec{k}_2 + 2\vec{k}_3 + \vec{k}_4) \end{cases}$$

In all of our simulations, we set our time step to be $\Delta \tilde{t} = 0.05$. If we set it larger than this, the sheet starts twisting and deforming in odd places. If we set it smaller than this, there is no discernible improvement in simulation quality.

4. Interpolating New Vortices

We start with only 1000 point vortices. Since this is not enough vortices to accurately represent the position of the vortex sheet as time progresses, we used a 3rd-order Lagrange interpolation formula for placing new vortices into the vortex sheet as time progresses, interpolating on the α variable. For four pre-existing sequential points

$$\begin{cases} \vec{x}_{k-2} = \vec{x}(\alpha_{k-2}, \tilde{t}) \\ \vec{x}_{k-1} = \vec{x}(\alpha_{k-1}, \tilde{t}) \\ \vec{x}_k = \vec{x}(\alpha_k, \tilde{t}) \\ \vec{x}_{k+1} = \vec{x}(\alpha_{k+1}, \tilde{t}) \end{cases}$$

we insert a new point $\vec{x}_k = \vec{x}(\alpha_k, \tilde{t})$ as follows;

$$\vec{x}_{k+1} \rightarrow \vec{x}_{k+2}, \vec{x}_k \rightarrow \vec{x}_{k+1}, \alpha_{k+1} \rightarrow \alpha_{k+2}, \alpha_k \rightarrow \alpha_{k+1}, \alpha_k = \frac{\alpha_{k-1} + \alpha_{k+1}}{2}; K+1 \rightarrow K$$

$$\begin{aligned} \vec{x}_k \approx & \vec{x}_{k-2} \left(\frac{(\alpha_k - \alpha_{k-1})(\alpha_k - \alpha_{k+1})(\alpha_k - \alpha_{k+2})}{(\alpha_{k-2} - \alpha_{k-1})(\alpha_{k-2} - \alpha_{k+1})(\alpha_{k-2} - \alpha_{k+2})} \right) + \vec{x}_{k-1} \left(\frac{(\alpha_k - \alpha_{k-2})(\alpha_k - \alpha_{k+1})(\alpha_k - \alpha_{k+2})}{(\alpha_{k-1} - \alpha_{k-2})(\alpha_{k-1} - \alpha_{k+1})(\alpha_{k-1} - \alpha_{k+2})} \right) \\ & + \vec{x}_{k+1} \left(\frac{(\alpha_k - \alpha_{k-2})(\alpha_k - \alpha_{k-1})(\alpha_k - \alpha_{k+2})}{(\alpha_{k+1} - \alpha_{k-2})(\alpha_{k+1} - \alpha_{k-1})(\alpha_{k+1} - \alpha_{k+2})} \right) + \vec{x}_{k+2} \left(\frac{(\alpha_k - \alpha_{k-2})(\alpha_k - \alpha_{k-1})(\alpha_k - \alpha_{k+1})}{(\alpha_{k+2} - \alpha_{k-2})(\alpha_{k+2} - \alpha_{k-1})(\alpha_{k+2} - \alpha_{k+1})} \right) \end{aligned}$$

We use this formula to insert new point vortices under the following criteria:

- 1) if the new point would be between the two outermost inflection points,
- 2) if the new point would not be between the two outermost points of sharply changing curvature, and
- 3) if the new point would make a vortex loop contain more than a defined minimum of points.

We impose the first two criteria in order to reduce the number of points we must keep track of during later time steps; this conserves computation time. We impose the final criterion to visually refine the vortex loops on either side of the vortex sheet.

a. *Inflection Point Criterion*

We only interpolate on points between the two outermost inflection points of the vortex sheet, in order to conserve some computation time. To determine these points, we calculate the z-component (since these are 2-dimensional vectors, the x- and y-components of their cross product are always zeroes) of the cross product of the resultant vectors made by two adjacent sets of two vortices each (three vortices total), and we restrict the interpolation scheme to operate only between the vortices where these sequential cross products change sign, either from positive to negative or vice versa. We calculate the z-component of the cross products as follows;

From left,

$$\begin{aligned} \vec{r}_k &= (\tilde{x}_k - \tilde{x}_{k-1}, \tilde{y}_k - \tilde{y}_{k-1}, 0); \\ \vec{r}'_k &= (\tilde{x}_{k+1} - \tilde{x}_k, \tilde{y}_{k+1} - \tilde{y}_k, 0); \\ \vec{r}_k \times \vec{r}'_k &= \begin{vmatrix} \hat{x} & \hat{y} & \hat{z} \\ \tilde{x}_k - \tilde{x}_{k-1} & \tilde{y}_k - \tilde{y}_{k-1} & 0 \\ \tilde{x}_{k+1} - \tilde{x}_k & \tilde{y}_{k+1} - \tilde{y}_k & 0 \end{vmatrix} = (0, 0, [(\tilde{x}_k - \tilde{x}_{k-1})(\tilde{y}_{k+1} - \tilde{y}_k) - (\tilde{y}_k - \tilde{y}_{k-1})(\tilde{x}_{k+1} - \tilde{x}_k)]) \end{aligned}$$

From right,

$$\begin{aligned} \vec{r}_k &= (\tilde{x}_k - \tilde{x}_{k+1}, \tilde{y}_k - \tilde{y}_{k+1}, 0); \\ \vec{r}'_k &= (\tilde{x}_{k-1} - \tilde{x}_k, \tilde{y}_{k-1} - \tilde{y}_k, 0); \\ \vec{r}_k \times \vec{r}'_k &= \begin{vmatrix} \hat{x} & \hat{y} & \hat{z} \\ \tilde{x}_k - \tilde{x}_{k+1} & \tilde{y}_k - \tilde{y}_{k+1} & 0 \\ \tilde{x}_{k-1} - \tilde{x}_k & \tilde{y}_{k-1} - \tilde{y}_k & 0 \end{vmatrix} = (0, 0, [(\tilde{x}_k - \tilde{x}_{k+1})(\tilde{y}_{k-1} - \tilde{y}_k) - (\tilde{y}_k - \tilde{y}_{k+1})(\tilde{x}_{k-1} - \tilde{x}_k)]) \end{aligned}$$

b. *Loop Criterion*

We determine whether a vortex loop contains enough points by examining two adjoining points on the

vortex sheet, computing what angle they make with the center of the vortex loops (taken here to be the outermost inflection points, as calculated above), and placing a new point between them if this angle is not sufficiently large. Computationally, we cut off the interpolation scheme if the cosine of this angle is too large; we use the Law of Cosines to calculate the angle. We use an angle of $\pi/30$ for a cutoff; a smaller angle would make the computation run too long, and a larger angle would detract from our ability to visualize the vortex loops.

$$\begin{aligned}
A_1 &= \sqrt{(\tilde{x}_{k-1} - \tilde{x}_l)^2 + (\tilde{y}_{k-1} - \tilde{y}_l)^2}; \\
A_2 &= \sqrt{(\tilde{x}_{k-1} - \tilde{x}_r)^2 + (\tilde{y}_{k-1} - \tilde{y}_r)^2}; \\
B_1 &= \sqrt{(\tilde{x}_k - \tilde{x}_l)^2 + (\tilde{y}_k - \tilde{y}_l)^2}; \\
B_2 &= \sqrt{(\tilde{x}_k - \tilde{x}_r)^2 + (\tilde{y}_k - \tilde{y}_r)^2}; \\
C &= \sqrt{(\tilde{x}_k - \tilde{x}_{k-1})^2 + (\tilde{y}_k - \tilde{y}_{k-1})^2}; \\
\cos \theta_1 &= \frac{A_1^2 + B_1^2 - C^2}{2 A_1 B_1}; \quad \cos \theta_2 = \frac{A_2^2 + B_2^2 - C^2}{2 A_2 B_2}
\end{aligned}$$

where $(\tilde{x}_l, \tilde{y}_l)$ is the location of the left inflection point, and $(\tilde{x}_r, \tilde{y}_r)$ is the location of the right inflection point.

c. *Sharp Curvature Criterion*

We determine whether the curvature κ is changing too sharply by calculating $d\kappa/d\alpha$, and cutting off the interpolation scheme from the leftmost point this occurs to the rightmost point. We use $d\kappa/d\alpha = 100000$ for a cutoff; much lower than this, the curvature criterion cuts off too many points to be useful; much higher than this, the curvature criterion fails to cut off any more points. Taking the variable s to be arc length, we calculate the curvature as follows;

$$\kappa = \left| \frac{d^2 \vec{R}}{d s^2} \right|; \quad \frac{d \kappa}{d \alpha} = \frac{d}{d \alpha} \left| \frac{d^2 \vec{R}}{d s^2} \right|$$

or, discretely (using formulas for finite-difference derivative approximations),

$$\begin{aligned}
{}_1\Delta s_k &= \sqrt{(\tilde{x}_k - \tilde{x}_{k-1})^2 + (\tilde{y}_k - \tilde{y}_{k-1})^2}; \\
{}_2\Delta s_k &= \sqrt{((\tilde{x}_{k+1} - \tilde{x}_k)^2 + (\tilde{y}_{k+1} - \tilde{y}_k)^2)}; \\
\kappa_k &= 2 \frac{\sqrt{[{}_1\Delta s_k (\tilde{x}_{k+1} - \tilde{x}_k) - {}_2\Delta s_k (\tilde{x}_k - \tilde{x}_{k-1})]^2 + [{}_1\Delta s_k (\tilde{y}_{k+1} - \tilde{y}_k) - {}_2\Delta s_k (\tilde{y}_k - \tilde{y}_{k-1})]^2}}{({}_1\Delta s_k {}_2\Delta s_k ({}_1\Delta s_k + {}_2\Delta s_k))} \quad \forall k = [1, K-1];
\end{aligned}$$

$$\kappa_0 = \kappa_1; \quad \kappa_K = \kappa_{K-1};$$

$$\left. \frac{d \kappa}{d \alpha} \right|_k = \frac{\kappa_{k+1} - \kappa_{k-1}}{\alpha_{k+1} - \alpha_{k-1}} \quad \forall k = [1, K-1];$$

$$\left. \frac{d \kappa}{d \alpha} \right|_0 = \frac{\kappa_1 - \kappa_0}{\alpha_1 - \alpha_0}; \quad \left. \frac{d \kappa}{d \alpha} \right|_K = \frac{\kappa_K - \kappa_{K-1}}{\alpha_K - \alpha_{K-1}}$$

5. *Weight Correction*

After we have interpolated all the new points we need per time step, we re-adjust the circulation strengths of these new points, before we begin the next time step, as follows;

$$\Delta \tilde{\Gamma}_k = w_k \cdot \Delta \alpha_k = \frac{d \tilde{\Gamma}}{d \alpha} \Big|_k \cdot \Delta \alpha_k = \cos(\alpha_k) \cdot \Delta \alpha_k;$$

$$\Delta \alpha_0 = \frac{\alpha_1 - \alpha_0}{2}; \Delta \alpha_K = \frac{\alpha_K - \alpha_{K-1}}{2}; \Delta \alpha_k = \frac{\alpha_{k+1} - \alpha_{k-1}}{2} \quad \forall k = [1, K-1]$$

Although this formula is slightly different from the initialization formula presented in §III.C.1., it renders virtually the same result of $\cos(\alpha_k) \cdot \Delta \alpha_k$, differing by an amount we take to be negligible.

E. Two Vortex Approximation

After we complete a run of the simulation for many vortices, we approximate the motion again for only two vortices, placed as follows using the center-of-mass formula;

$$\tilde{x}_l = \frac{\sum_{k=0}^{(K-1)/2} \tilde{x}_k \Delta \tilde{\Gamma}_k}{\sum_{k=0}^{(K-1)/2} \Delta \tilde{\Gamma}_k}; \tilde{x}_r = \frac{\sum_{k=(K+1)/2}^K \tilde{x}_k \Delta \tilde{\Gamma}_k}{\sum_{k=(K+1)/2}^K \Delta \tilde{\Gamma}_k}; \tilde{\Gamma}_l = 1; \tilde{\Gamma}_r = -1$$

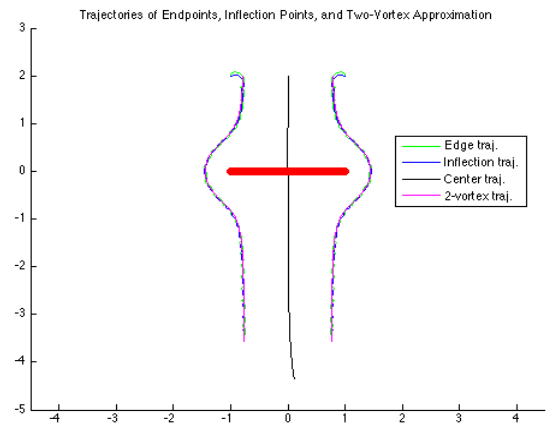
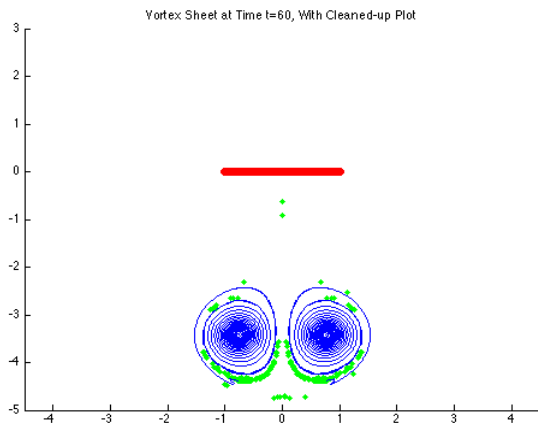
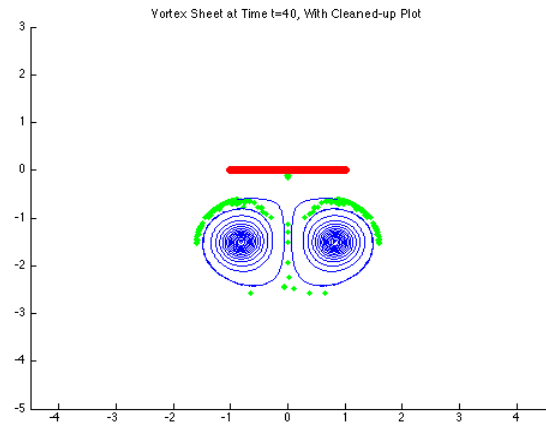
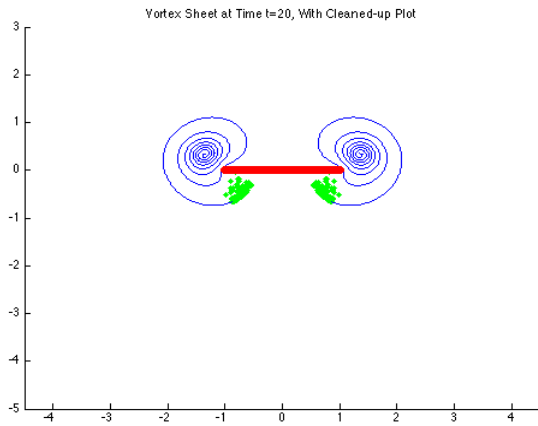
We then step forward in time as above, but we do not interpolate any points in between these two—we only track their position.

IV. Results

We track the vortex sheet's shape, the location of its endpoints, its outermost inflection points (which we take to be a close approximation of the vortex centers), and its initial center point, all as time progresses from $\tilde{t}=0$ to $\tilde{t}=60$.

A. Basic

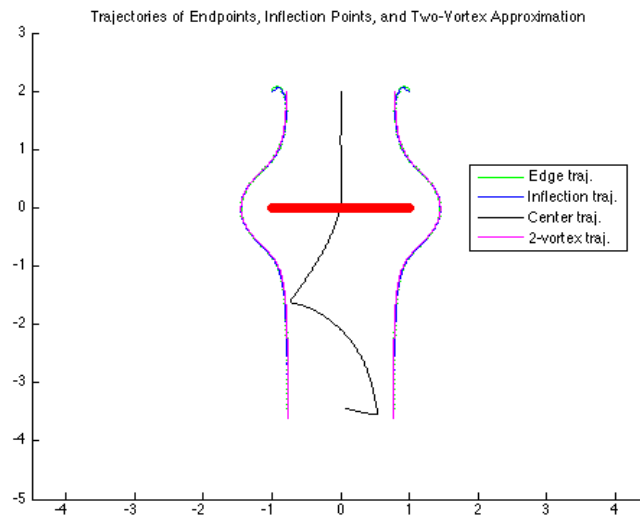
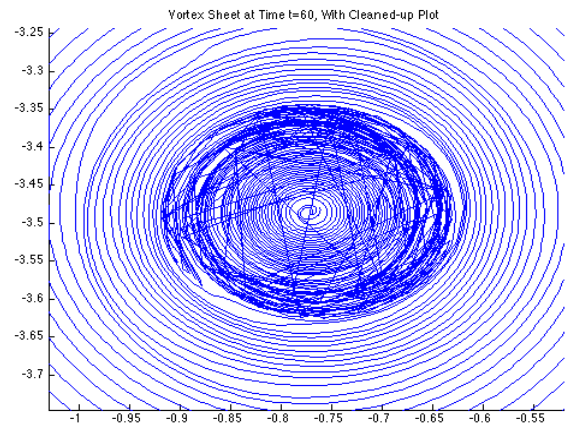
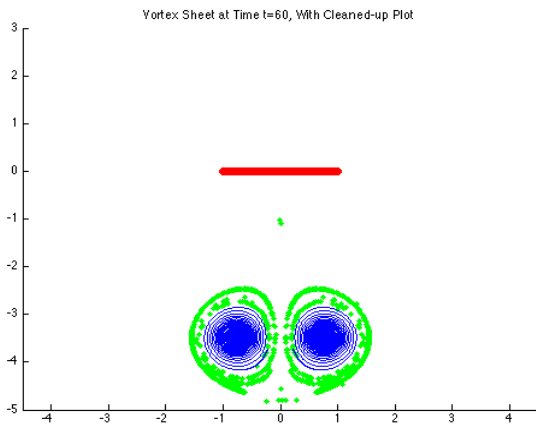
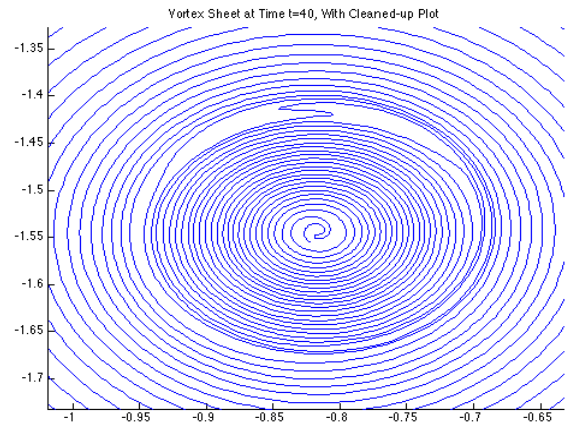
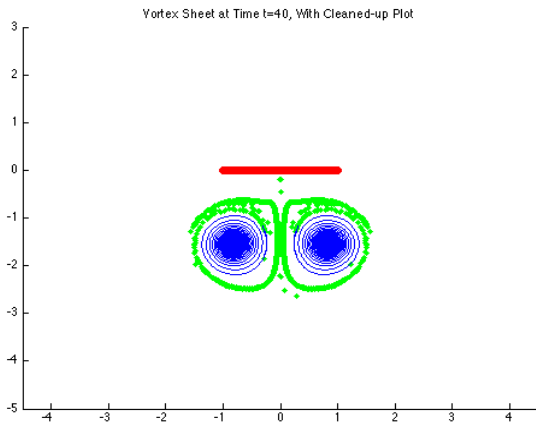
When we start with a basic set of parameters ($\delta = 0.2$, $d = 2$, $\varphi = 0$), we get the following results;



As we can see, the vortex sheet starts at the top and flows downward. The centers of the vortex loops wrap around the plate, then continue straight downward after they clear said plate. The edges of the vortex sheet follow these points closely, oscillating about the path of the vortex loops. The center segment of the vortex sheet veers slightly ahead and to the right at large times; we do not know why. (Computational error may be to blame, but we cannot be sure at this stage.)

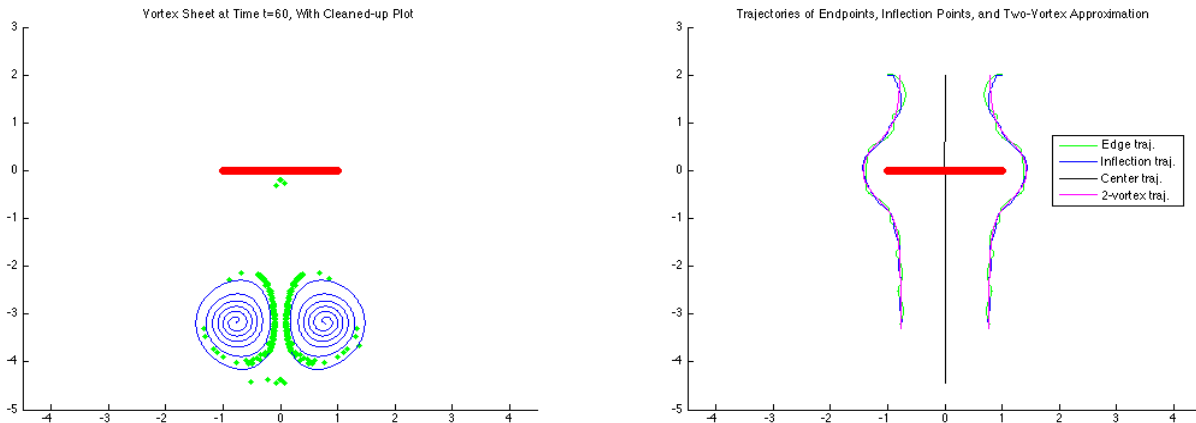
B. Variations

First, we vary the δ parameter. For $\delta = 0.1$ (half the original), we get the following results;



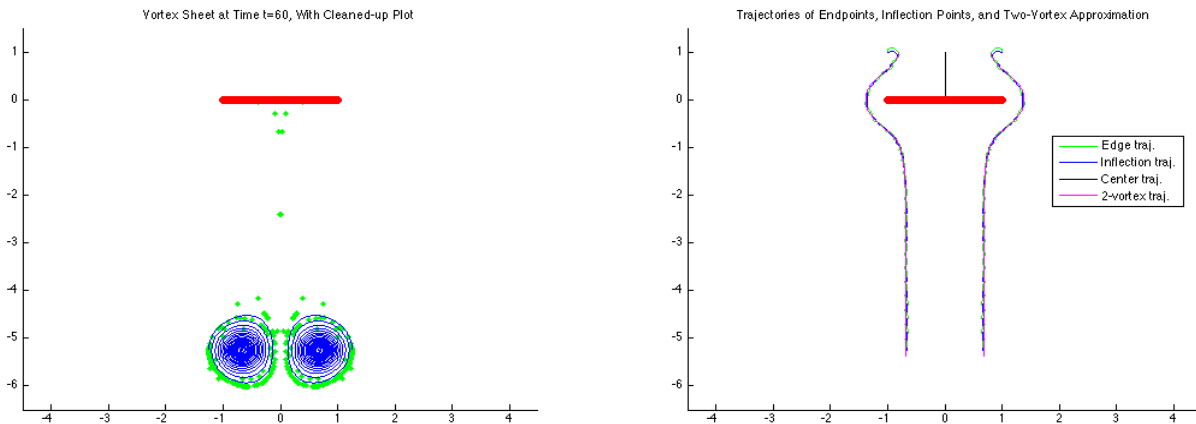
As before, the vortex sheet starts at the top and flows downward. The centers of the vortex loops wrap around the plate, then continue straight downward after they clear said plate. Starting at about $\tilde{t}=40$, the inner turns of the vortex loops exhibit unusual behavior; they start to loop backward, and they have broken apart by $\tilde{t}=60$. The reason for this behavior is uncertain. The edges of the vortex sheet follow the 2-vortex approximation paths closely and oscillate about the path of the vortex loops. After clearing the plate, the center segment of the vortex sheet veers to the left, then the right, then sharply left again.

For $\delta = 0.4$ (twice the original), we get the following results;



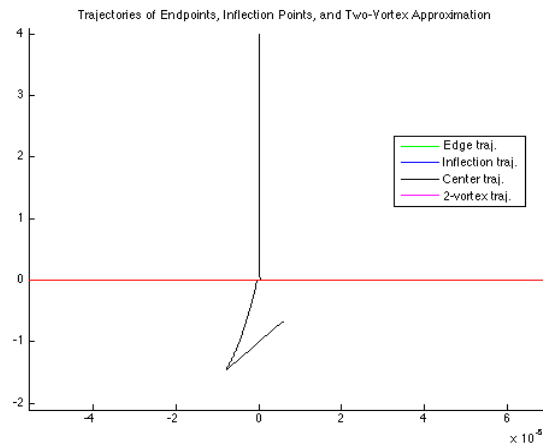
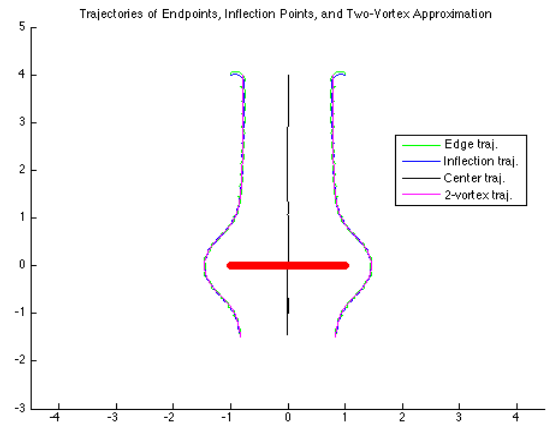
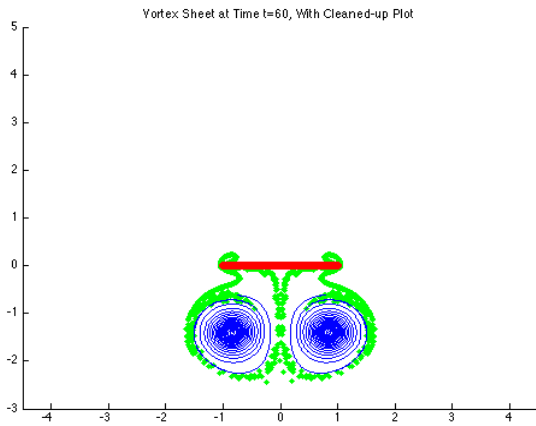
There are far fewer turns in the vortex loops for this run of the simulation. This time, the center line runs practically straight down, but the edge and inflection trajectories oscillate with a visibly greater amplitude than with lower values of δ .

Next, we vary the d parameter. For $d = 1$ (half the original), we get the following results;



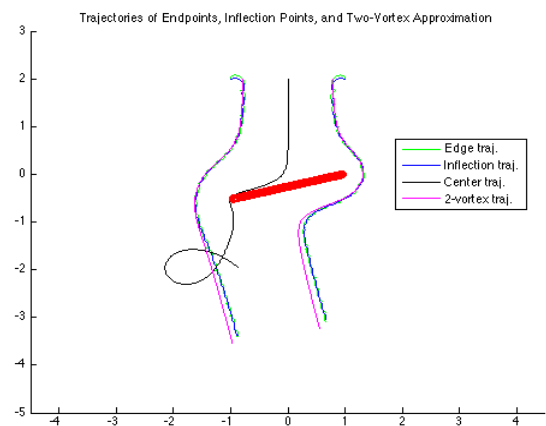
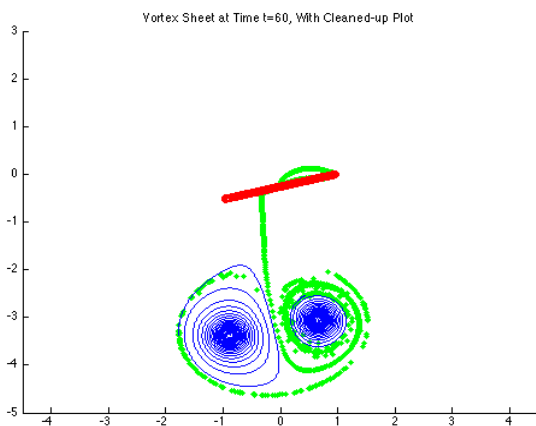
The vortex loops are more well defined for $d = 1$ than for the default $d = 2$. This time, the center element drops straight down to the plate and stops; it does not wrap around it as it does for the previously discussed runs. The vortex trajectories wrap around the plate then proceed straight downward, as they do in other runs.

For $d = 4$ (twice the original), we get the following results;



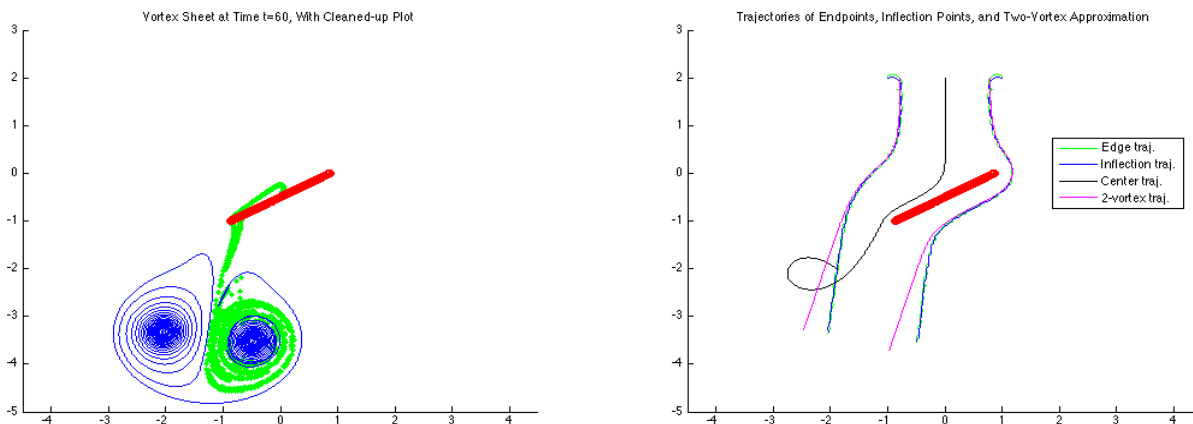
The vortex loops remain mostly well-defined, but the sheet behavior becomes very jagged closer to the plate, as the vortex sheet wraps around it. The vortex trajectories proceed straight downward, then they wrap around the plate. The endpoints and inflection points oscillate about their paths as they do in all other runs. The center-point trajectory goes mostly straight down, but in the last few time steps it backs up and goes almost straight upward.

Then, we vary the ϕ parameter. For $\phi = \pi/12$, we get the following results;



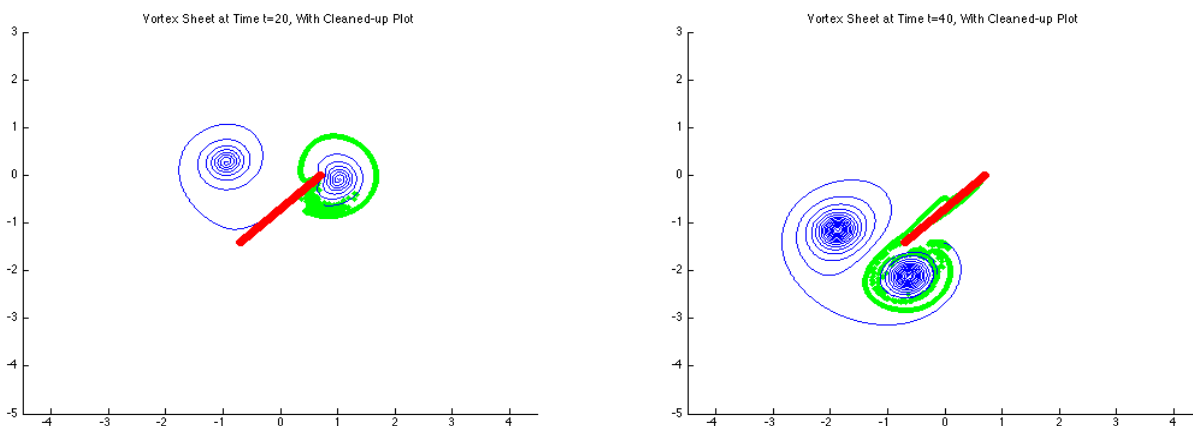
The vortex loop on the lower side of the plate remains well-defined, but the vortex loop on the higher side of the plate loses definition and has high curvature inside its turns. The vortex trajectories wrap around the plate, then continue outwards perpendicular to the plate, rather than straight down. The 2-vortex trajectories are slightly to the left of the endpoints and inflection points. The center point loops around to the left of the plate after it hits the plate.

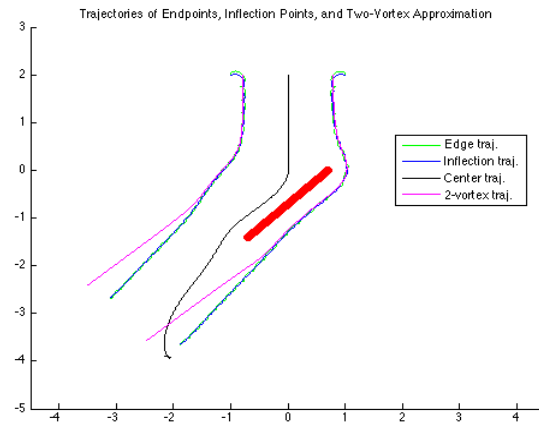
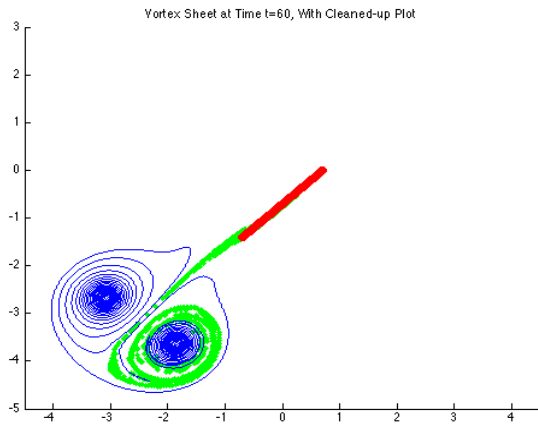
For $\varphi = \pi/6$, we get the following results;



The vortex loop on the lower side of the plate remains well-defined, but the vortex loop on the higher side of the plate loses definition and has high curvature inside its turns, just like when $\varphi = \pi/12$. The vortex trajectories wrap around the plate, then continue outwards down and to the left of the plate, rather than straight down. The 2-vortex trajectories are at a greater angle to the left of the endpoints and inflection-point trajectories. The center point loops around to the left of the plate after it hits the plate.

For $\varphi = \pi/4$, we get the following results;





The vortex loop on the upper-left side of the line made by the plate remains well-defined, but the vortex loop on the lower-right side of the line made by the plate loses definition and has higher curvature inside its turns, the same as other cases when $\varphi > 0$. The vortex trajectories wrap around the plate, then continue outwards almost parallel to the plate. The 2-vortex trajectories are at a slightly greater angle to the left of the endpoints and inflection-point trajectories, but they also continue outwards almost parallel to the plate. The center point turns left after it hits the plate, almost parallel to it, then continues downward, slowly turning straight downward, and even briefly veering right near the end of the run.

V. Summary

As we modify the parameters of the vortex sheet, we notice the following trends. As we shrink δ , the vortex sheet develops more turns, and for the smallest value of δ , these turns start to loop backward. However, the trajectories of the endpoints, inflection points, and two-vortex approximation points seem unchanged. As we modify d , we only notice that the vortex sheet crosses the plate at different times; its physical behavior otherwise seems largely unaffected. Again, the trajectories of the endpoints, inflection points, and two-vortex approximation points seem unchanged. However, these trajectories do change as we modify φ ; they seem to be deflected as the angle of the plate changes, although the exact relationship of the plate angle to the vortex deflection angle is uncertain.

VI. Bibliography

¹Nitsche, Monika and Krasny, Robert, "A numerical study of vortex ring formation at the edge of a circular tube," J. Fluid Mech. Vol. 276, pp. 139-161 (1994)

²Krasny, Robert, "A study of singularity formation in a vortex sheet by the point-vortex approximation," J. Fluid Mech. Vol. 167, pp. 65-93 (1986)

³Krasny, Robert, "Computation of vortex sheet roll-up in the Trefftz plane," J. Fluid Mech. Vol. 184, pp. 123-155 (1987)

⁴Krasny, Robert, "Desingularization of Periodic Vortex Sheet Roll-up" Journal of Computational Physics Vol. 65, pp 292-313 (1986)

⁵Nitsche, Monika, “Minicourse 4: An Introduction to Fluid Dynamics” (2008)

⁶Nitsche, Monika, “Scaling properties of vortex ring formation at a circular tube opening” Phys. Fluids Vol. 8 No. 7 (1996)

⁷Nitsche, Monika, “Vortex Dynamics”

⁸Pullin, D. I., private communication, 1983